# Theoretical study of the rhenium–alkane interaction in transition metal–alkane $\sigma$-complexes

Erika A. Cobar[†§¶], Rustam Z. Khaliullin[§¶], Robert G. Bergman[§¶‖], and Martin Head-Gordon[§¶]

[†]Laboratory of Computational Biology, Computational Biophysics Section, Heart, Lung, and Blood Institute, National Institutes of Health, Bethesda, MD 20892; [§]Department of Chemistry, University of California, Berkeley, CA 94720; and [¶]Chemical Sciences Division, Lawrence Berkeley National Laboratory, Berkeley, CA 94720

Edited by John E. Bercaw, California Institute of Technology, Pasadena, CA, and approved February 26, 2007 (received for review November 14, 2006)

**Metal–alkane binding energies have been calculated for [CpRe(CO)$_2$](alkane) and [(CO)$_2$M(C$_5$H$_4$)C≡C(C$_5$H$_4$)M(CO)$_2$](alkane), where M = Re or Mn. Calculated binding energies were found to increase with the number of metal–alkane interaction sites. In all cases examined, the manganese–alkane binding energies were predicted to be significantly lower than those for the analogous rhenium–alkane complexes. The metal (Mn or Re)–alkane interaction was predicted to be primarily one of charge transfer, both from the alkane to the metal complex (70–80% of total charge transfer) and from the metal complex to the alkane (20–30% of the total charge transfer).**

binding energy | C—H activation | DFT calculations | manganese

Carbon–hydrogen (C—H) bond activation reactions are important from a fundamental point of view, as well as in more practical terms to medicine, academia, and industry, as they are being used for the conversion of common, inexpensive alkanes into reactive (and physiologically active) molecules (1, 2). Many transition metal complexes are now known that can be used to activate C—H bonds in alkanes (3). With low-valent metal complexes, the first bond-breaking step involves oxidative addition of an alkane to an unsaturated metal center (Fig. 1). The goal of subsequent steps is to convert the alkyl group R into an alcohol ROH or other potentially useful functionalized organic molecule.

Many researchers today are focusing on the development of industrially practical organometallic oxidation catalysts (5–8), but there remain fundamental aspects of the C—H activation process that are not fully understood. For instance, it is widely accepted that C—H activation reactions proceed via alkane $\sigma$-complex intermediates (3) (Fig. 1, compound **3**), and such species have recently been detected and studied in low-temperature NMR experiments (9–11). Although complexes with intramolecular C—H/metal (so-called agostic) interactions have been isolated and crystallographically characterized (3), in systems where strong evidence has been provided for intermolecular metal–alkane coordination in solution (9–11), isolation and solid state structural characterization have not yet been accomplished.[††] Intermolecular metal–alkane complexes are therefore one of the most important targets in the study of C—H activation; an understanding of the mechanisms of C—H activation, which will allow researchers to better control and manipulate the outcome of the reactions, is crucial for the advancement of this area of chemistry.

Quantum chemical methods have become useful and practical tools in study of TM complexes (14–17). Particularly, advancements in density functional theory (DFT) (16) and the use of effective core potentials (14, 15) have made qualitatively accurate predictions of the structures and chemistry of TM complexes possible at a reasonable computational cost (17). The goals of the present work are twofold: to make computational predictions of the relative stabilities of a selection of alkane $\sigma$-complexes, which will aid synthetic chemists in their efforts toward isolating and fully characterizing such species, and to explain the nature of the alkane–metal interaction in such complexes.

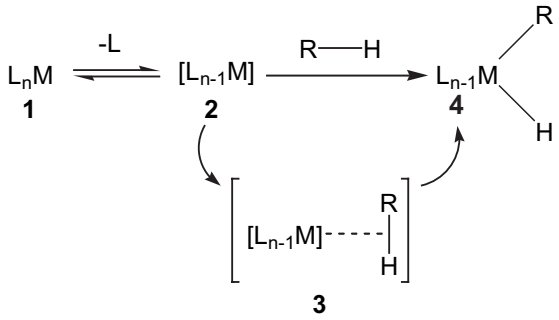


**Fig. 1.** Oxidative addition of an alkane RH to an unsaturated metal complex, 2, which is typically generated by photolysis of a saturated metal complex, 1. The reaction is proposed to proceed via an alkane $\sigma$-complex intermediate, 3. Figure was adapted from ref. 4.

## Background

A $\sigma$-complex is a transition metal complex in which a $\sigma$-bond acts as a ligand. Intermolecular $\sigma$-complexes of borohydrides, silanes, and dihydrogen have all been isolated and characterized; as mentioned above, intermolecular alkane $\sigma$-complexes have proven to be much more elusive to isolation. The existence of isolable $\sigma$-complexes of any type is surprising, because $\sigma$ bonds are far weaker electron donors than the lone pairs of more traditional ligands (e.g., amines, phosphines) or the $\pi$ bonds of $\pi$-bonding ligands (e.g., alkenes, alkynes). The stability of $\sigma$-complexes is attributed in large part to the proposed occurrence of electron back-donation from a filled metal d orbital into the $\sigma^*$ orbital; such back-bonding is thought to be necessary for strong binding to occur (5).

Some of the earliest evidence for alkane $\sigma$-complexes came from studies of the Group 6 metal carbonyls. Photolysis of M(CO)$_6$ (M = Cr, Mo, W) produces M(CO)$_5$ fragments, which were shown, first by low-temperature UV/VIS (18, 19), and later

Author contributions: E.A.C., R.G.B., and M.H.-G. designed research; E.A.C. and R.Z.K. performed research; E.A.C., R.Z.K., R.G.B., and M.H.-G. analyzed data; and E.A.C. and R.Z.K. wrote the paper.

The authors declare no conflict of interest.

This article is a PNAS Direct Submission.

Abbreviations: TM, transition metal; DFT, density functional theory; BE, binding energy; ALMO, absolutely localized molecular orbital; EDA, energy decomposition analysis.

‖To whom correspondence should be addressed. E-mail: rbergman@berkeley.edu

[††]Two X-ray structures have been published of complexes in which alkanes are located in the proximity of metal centers (12, 13). However, in neither of these cases is the alkane metal-coordinated in solution.

This article contains supporting information online at www.pnas.org/cgi/content/full/0610295104/DC1.

by photoacoustic calorimetry (20–23) and gas-phase TRIR (24), to bind single alkane molecules as sixth ligands. The magnitude of the $M(CO)_5$(alkane) interaction is on the order of 10 kcal/mol (20–24).

As mentioned above, alkane $\sigma$-complexes are also believed to be intermediates in the activation of C—H bonds by transition metal complexes. Early evidence for the presence of C—H $\sigma$-complexes in C—H activation reactions was provided by isotopic labeling NMR experiments on the reversible oxidative addition of cyclohexane to $Cp^*IrPMe_3$ (25). In these experiments (25), and others similar to them (26–29), an inverse kinetic isotope effect and H/D exchange between the hydride and alkyl groups before elimination of the alkane indicated the presence of an alkane $\sigma$-complex intermediate. More recently, direct evidence for alkane $\sigma$-complex intermediates was obtained from TRIR flash kinetics studies on the photoinduced C—H bond activation by $Cp^*Rh(CO)_2$ in liquid rare gases (30–32). These experiments showed a reaction intermediate, assigned to be $Cp^*Rh(CO)$(alkane), which became increasingly stable (relative to the reactants) with increasing alkane size, ranging from −0.9 kcal/mol for ethane to −2.3 kcal/mol for octane and from −2.4 kcal/mol for cyclopentane to −3.5 kcal/mol for cyclooctane (32). Also studied was the reaction profile of methane activation by $CpRe(CO)_2$ using computational methods, which predicted a methane $\sigma$-complex intermediate lying 8.7 kcal/mol below reactants in enthalpy, with an activation barrier to C—H oxidative addition of 6.6 kcal/mol (33).

The present work focuses not on achieving C—H activation, but on optimizing the stability of the proposed alkane $\sigma$-complex intermediate species. The goal in designing an isolable alkane $\sigma$-complex should be to choose the combination of metal, ligands, and alkane that is the most thermodynamically stable with respect to reactants and that has the highest barrier to oxidative addition. Inspection of existing experimental and theoretical evidence provides guidance in the design of such a complex. Using solution-phase TRIR spectroscopy, Childs *et al.* revealed a trend that is critical to the choice of metal center (34, 35). The group studied the reaction of complexes of the form $CpM(CO)_x$(*n*-heptane) with CO, and found that the rate of displacement of *n*-heptane by CO decreased with the identity of M both across and down Groups 5, 6, and 7 of the periodic table. The difference between the two extremes (top of Group 5 vs. bottom of Group 7) was remarkable; $CpV(CO)_3$(*n*-heptane) reacted 50,000 times more rapidly than $CpRe(CO)_2$(*n*-heptane). Also, for the choice of alkane, experiment indicates that large alkanes form more stable complexes than smaller alkanes, and that cyclic alkanes form more stable complexes than comparably sized linear alkanes (24, 32, 35). In agreement with the observed stability trends, several rhenium complexes with rather large alkanes, $CpRe(CO)_2$-(cyclopentane), -(cyclohexane), and -(*n*-pentane), have now been detected using low-temperature NMR (9–11).

The present study takes its lead from experimental evidence and investigates the stability of a series of $CpRe(CO)_2$(alkane) complexes, as well as that of several proposed but so far unknown binuclear analogs, $[(CO)_2Re(C_5H_4)C{\equiv}C(C_5H_4)Re(CO)_2]$(alkane) (Fig. 2). Binding energies (BE) for selected examples of the manganese analogs of the complexes were also calculated to compare the alkane-binding capability of rhenium with that of a lighter Group 7 metal. The reported binding energies were calculated by using DFT with the Becke–Perdew 1986 (BP86) functional (36, 37).

## Results and Discussion

**Supporting Information.** For further details, see supporting informaiton (SI) *Appendix*, SI Tables 3–11, and SI Figs. 8–11.

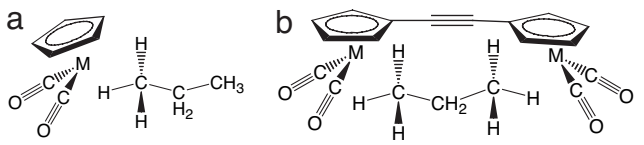


**Fig. 2.** The mononuclear and binuclear alkane $\sigma$-complexes examined in this work, $CpM(CO)_2$(alkane) (*a*) and $[(CO)_2M(C_5H_4)C{\equiv}C(C_5H_4)M(CO)_2]$ (*b*), M = Re or Mn.

**Mononuclear Binding Energies.** For the mononuclear complexes, $CpM(CO)_2$(alkane), it was initially assumed that the binding in the *n*-alkane $\sigma$-complexes would occur at one of the terminal C—H bonds; this is a reasonable assumption, because it is the terminal carbon that is activated in the C—H activation reactions of related transition metal complexes. However, a recently published experiment brought the validity of that assumption into question. Ball *et al.* (10) found that in solution, $(i\text{-}Pr(C_5H_4))Re(CO)_2$(pentane) actually exists in three forms: $(i\text{-}Pr(C_5H_4))Re(CO)_2$(1-pentane), $(i\text{-}Pr(C_5H_4))Re(CO)_2$(2-pentane), and $(i\text{-}Pr(C_5H_4))Re(CO)_2$(3-pentane) in a ratio of 6:6.07:2.9. When compared with a statistical ratio of 6:4:2, this observed ratio corresponds to a thermodynamic preference of 0.13 kcal/mol for $CH_2$ binding over $CH_3$ binding. Also, Vetter *et al.* (38) observed a 1.5× kinetic preference for coordination at a secondary C—H bond rather than at a primary C—H bond for Tp′RhL(alkane) complexes (Tp′=Tris-(3,5-dimethylpyrazolyl) borate; L=$CNCH_2CMe_3$).

Binding energies at all possible interaction sites were calculated for the *n*-pentane and *n*-heptane $CpRe(CO)_2$ complexes (SI Table 3). The metal–alkane interaction strength was predicted to be larger by ≈1 kcal/mol when the interaction site was one of the terminal $CH_3$ groups (Fig. 2*a*) than when it was any of the secondary $CH_2$ groups (SI Table 3). This prediction is in disagreement with the slight thermodynamic preference (0.13 kcal/mol) for binding at secondary carbons observed by NMR (10). Differences between our calculations and solution-phase experimental results are to be expected because, in addition to their intrinsic errors, our calculations produce an estimate of gas-phase enthalpy, and do not account for changes in entropy or for the effects of solvation (which we expect to be small). There are also structural differences between the *in silico* and *in situ* experiments, which should be considered when comparing the two sets of results: the experimental structures contain $i\text{-}Pr(C_5H_4)$ or Tp′ instead of Cp as a ligand. In any case, the linear alkane binding energies presented as final results in this work were calculated for the interaction of the metal center with the terminal $CH_3$ group (Fig. 3). Binding energies were also calculated for a series of cyclic alkanes (Fig. 3).

Several geometrical parameters were examined for each of the optimized mononuclear complexes (SI Table 5). For these complexes, only one C—H bond of the interacting $CH_2$(cyclic alkanes)/$CH_3$(linear alkanes) group participates in the binding. The interaction is best described as an asymmetric $\eta^2$-C, H type (Fig. 4*d*), in which the H atom lies closer to the metal atom M than does the C atom. An illustration of the optimized methane complex is provided as a representative example of the binding (Fig. 5). The M–H–C angles range from 112° to 122° (SI Table 5), the M–C distances from 2.58 Å to 2.72 Å, and the M-H distances from 1.91 Å to 1.97 Å (SI Table 5). The interacting C—H bond is elongated by 0.06–0.07 Å relative to the free C—H bonds on the same $CH_2/CH_3$ group (SI Table 5).

For the linear alkane complexes, the ethane to *n*-heptane (C2–C7) predicted binding energies are all fairly similar. The largest difference in binding energy is seen in comparing methane to ethane or any of the multicarbon alkanes. It appears that the presence of a $CH_2/CH_3$ group adjacent to the interacting $CH_3$

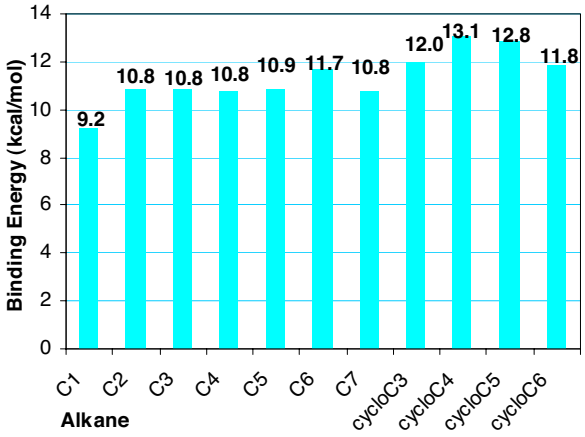


**Fig. 3.** Mononuclear rhenium [[CpRe(CO)$_2$](alkane)] binding energies, calculated at the BP86/6–31G*, LANL2DZ level of theory. C1, C2, C3, C4, C5, C6, and C7 represent methane, ethane, *n*-propane, *n*-butane, *n*-pentane, *n*-hexane, and *n*-heptane, respectively. cycloC3, cycloC4, cycloC5, and cycloC6 represent cyclopropane, cyclobutane, cyclopentane, and cyclohexane, respectively.

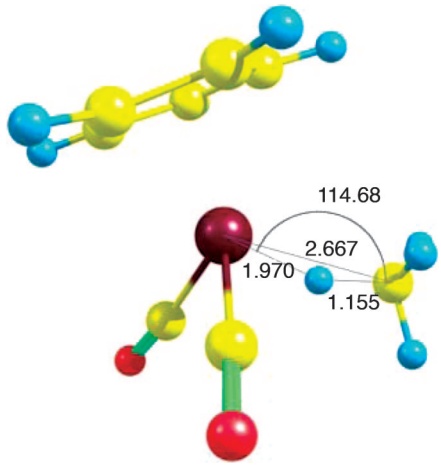


**Fig. 5.** Optimized [CpRe(CO)$_2$](methane) structure, calculated at the BP86/6-31G*, LANL2DZ level of theory. Bond lengths are provided in angstroms, bond angles are provided in degrees.

group significantly increases the metal–alkane interaction strength, but that further lengthening of the alkane chain has a much smaller effect.

The cyclopropane, cyclobutane, and cyclopentane binding energies are larger than those of their linear counterparts, and the cyclohexane value is roughly equal to that of *n*-hexane. The cyclobutane BE is the largest overall for the mononuclear complexes.

The reactivity of the mononuclear complexes [CpM(CO)$_2$](alkane), M = Mn or Re; alkane = *n*-heptane or cyclopentane have been investigated using infrared (IR) detection (39, 40). In the IR studies, the authors report enthalpies of activation ($\Delta H^{\ddagger}$) for the replacement of the coordinating alkane by a CO molecule. The $\Delta H^{\ddagger}$ values can be taken as lower limits of the strength of the metal complex–alkane interaction. They can serve as a rough check of the accuracy of the magnitudes of our computational values, and in this sense, they are in good agreement. The experimental values for $\Delta H^{\ddagger}$ are 13.6 kcal/mol (39) and 11.0 kcal/mol (40) for [CpRe(CO)$_2$](*n*-heptane) and 7.7 kcal/mol for [CpRe(CO)$_2$](cyclopentane); our respective calculated values are 10.8 kcal/mol and 12.8 kcal/mol.

The ultimate goal of our work is to find an alkane $\sigma$-complex that would be stable enough to isolate and fully characterize; we estimate that the binding enthalpy that this would require would be on the order of 30 kcal/mol. The mononuclear [[CpRe(CO)$_2$](alkane)] binding energies, whether predicted by computation or reported from experiment are too small to allow for isolation of these complexes at a reasonable temperature. For this reason, we chose to investigate their binuclear analogs, which could have significantly larger binding energies.

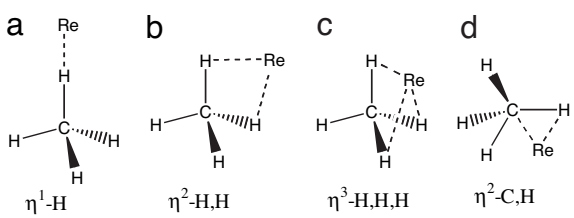


**Fig. 4.** Four possible binding modes for alkane $\sigma$-complexes, shown here for methane.

**Binuclear Binding Energies.** The calculated binuclear rhenium binding energies are indeed significantly larger than those of their mononuclear counterparts (Fig. 6). The binuclear structures for ethane (Fig. 7), *n*-propane, *n*-butane (Fig. 7), *n*-pentane, cyclopropane, cyclopentane, and cyclohexane all show two alkane–metal interaction sites (*SI Appendix*), and it is the presence of this second metal–alkane interaction that increases the binding energies so significantly. This conclusion is further supported by the two exceptions to this trend, which do not show a significant increase in binding energy with the presence of a second metal center: methane and cyclobutane (Fig. 6). Methane and cyclobutane are predicted to interact significantly with only one rhenium atom of the binuclear complexes (*SI Appendix*).

The binding observed at each of the two binding sites in the binuclear complexes is comparable to that observed at the mononuclear ([CpRe(CO)$_2$](alkane)) interaction sites; it is of the asymmetric $\eta^2$-C, H type, and the M–H and M–C bond

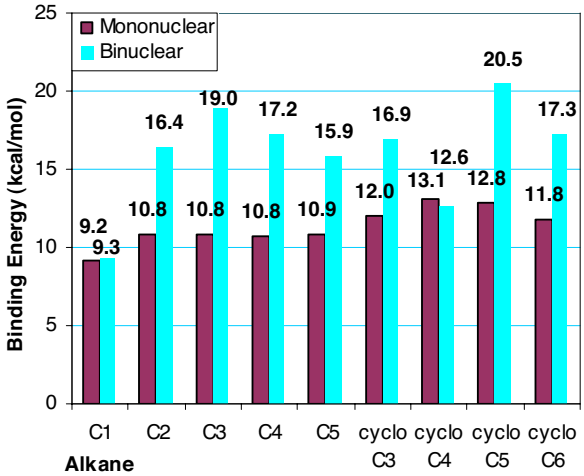


**Fig. 6.** Mononuclear rhenium ([CpRe(CO)$_2$](alkane)) binding energies and binuclear rhenium [[(CO)$_2$Re(C$_5$H$_4$)C≡C(C$_5$H$_4$)Re(CO)$_2$](alkane)] binding energies, all calculated at the BP86/6–31G*, LANL2DZ level of theory. C1, C2, C3, C4, C5, C6, and C7 represent methane, ethane, *n*-propane, *n*-butane, *n*-pentane, *n*-hexane, and *n*-heptane, respectively. cycloC3, cycloC4, cycloC5, and cycloC6 represent cyclopropane, cyclobutane, cyclopentane, and cyclohexane, respectively.

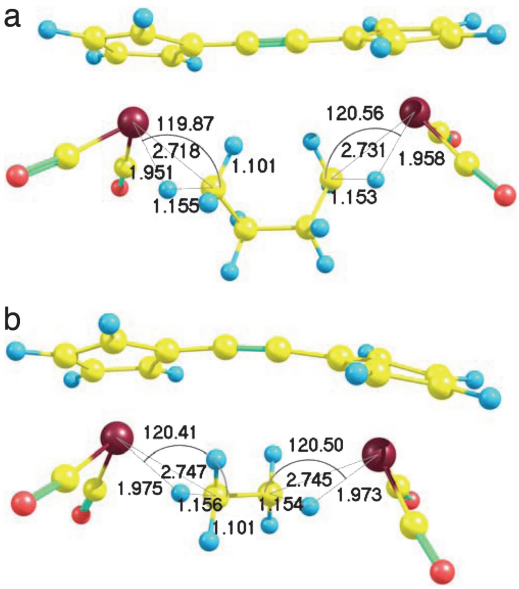


**Fig. 7.** Optimized $[(CO)_2Re(C_5H_4)C{\equiv}C(C_5H_4)Re(CO)_2](n\text{-butane})$ (*a*) and $[(CO)_2Re(C_5H_4)C{\equiv}C(C_5H_4)Re(CO)_2](\text{ethane})$ (*b*) structures, calculated at the BP86/6-31G*, LANL2DZ level of theory. Bond lengths are provided in angstroms, bond angles are provided in degrees.

distances and M–H–C angles are comparable to those seen in the optimized mononuclear complexes (SI Table 9).

For the mononuclear complexes, the binding energies were all fairly similar (Fig. 3). Lengthening of the alkane chain beyond two carbons had little effect on the magnitude of the binding energy. For the binuclear complexes, the length of the alkane chain is more important. The presence of one or two methylene spacers allows the terminal methyl groups of propane or butane to move freely, adopting a conformation in which their distances from the two metal centers are optimal for interaction (Fig. 7*a*). In the ethane complex, the two methyl groups have far less freedom, and to maximize their interaction with the two metal centers, the molecule can merely align itself between them (Fig. 7*b*). Accordingly, the binuclear ethane complex has both longer M–H and M–C distances (SI Table 9) and weaker binding than either the propane or butane complexes (Fig. 6).

Although it appears to be important for the terminal methyl groups of a linear alkane to have methylene spacers between them, too many methylene groups cause crowding, which limits the alkane's ability to adapt a favorable conformation for interaction with the metal complex. The pentane complex, for example, has larger M–H and M–C distances (SI Table 9) and a smaller binding energy than either the propane or butane complexes (Fig. 6). The *n*-propane molecule seems to strike a balance between flexibility and overall size, as it has the highest BE for the linear alkane complexes.

In the cyclic alkane complexes (excluding cyclobutane, which only interacts with one metal center), binding is predicted to occur with two adjacent carbons (*SI Appendix*). The calculated cyclopropane and cyclohexane structures both have larger M-H distances (SI Table 9) and smaller binding energies than the cyclopentane complex (Fig. 6). For cyclopropane, the reason for the difference may be that cyclopropane is limited in its ability to change conformation; the two interacting $CH_2$ groups are not able to rotate relative to each other, only to rigidly align themselves between the two metal centers. The cyclohexane molecule is more flexible than cyclopropane, but it appears to be simply too bulky to approach the metal centers as closely as cyclopentane is able to (*SI Appendix*).

**Table 1. Binuclear manganese and rhenium ($[(CO)_2M(C_5H_4)CsC(C_5H_4)M(CO)_2]$(alkane)) binding energies (kcal/mol), calculated at the BP86/6–31G*, LANL2DZ level of theory**

| | Manganese | Rhenium |
|---|---|---|
| Ethane | 8.0 | 16.4 |
| *n*-Propane | 12.7 | 19.0 |
| *n*-Butane | 12.1 | 17.2 |
| *n*-Pentane | 10.5 | 15.9 |

As discussed above, the binuclear complexes display much geometrical flexibility. The CO and Cp groups on each metal center are able to rotate relative to the groups on the other metal center, and the alkane molecules have many possible conformations that allow them to interact with the metal centers. Complexes with such extensive flexibility are likely to have complicated potential energy surfaces with many local minima, some of which may be close in energy. The binuclear structures presented in this work are thus most likely only local minima on the potential energy surfaces of the complexes. The mononuclear structures are also likely to have many local minima, close in energy to each other. If the complexes reported in this work are indeed local minima, then the results presented here are slight underestimates of the maximum calculated interaction strengths, which would occur at the global minima. The regularity in trends of the predicted BEs for each series of complex–alkane combinations suggests that the structures presented in this work are reasonable representations, which are not likely to vary greatly from other favorable interaction modes that may exist. The geometry guesses that were used as the inputs for the initial optimizations of the mono- and binuclear complexes are shown in *SI Appendix*.

Several binuclear manganese complexes were also examined. The work of Childs *et al.* showed that manganese complex–alkane adducts are much less stable than their rhenium analogs (34, 35). In agreement with experiment, the calculated manganese binding energies are significantly lower than those of their rhenium analogs (Table 1).

**Nature of the Alkane–Metal Bond.** Absolutely localized molecular orbital (ALMO) energy decomposition analysis (EDA) calculations (41) were used to analyze the nature of the alkane–metal bond in the complexes presented in this work. The ALMO EDA separates the total interaction energy ($\Delta E_{TOT}$) into four contributions: the geometric distortion energy needed to bring the fragments to their complex geometries ($\Delta E_{GD}$), the frozen density interaction energy ($\Delta E_{FRZ}$), the intramolecular orbital relaxation energy associated with the polarization of the metal complex and the alkane by each other ($\Delta E_{POL}$), and the intermolecular orbital relaxation energy associated with the charge transfer between the metal complex and the alkane ($\Delta E_{CT}$). The last term can be separated into two components: the energy lowering due to charge transfer from the metal complex to the alkane ($\Delta E_{M\rightarrow A}$), and the energy lowering due to the charge transfer from the alkane to the metal complex ($\Delta E_{A\rightarrow M}$). The $\Delta E_{M\rightarrow A}$ term provides a qualitative measure of the backbonding contribution to the interaction energy. The ALMO EDA results for the mononuclear manganese and rhenium complexes with methane, *n*-heptane, and cyclobutane are presented in Table 2.

The analyses show that the major contribution to binding between the alkane and the metal center is charge transfer (≈80% of the total favorable binding contributions), whereas the polarization contribution is less significant (≈20%) and the frozen density interaction is repulsive (Table 2). Between 70 and 80% of the $\Delta E_{CT}$ is associated with charge transfer from the

**Table 2. BP86/6-31G*, LANL2DZ EDA results for the mononuclear rhenium complexes of methane, *n*-heptane, and cyclobutane, optimized at the same level of theory**

| | Re | | | Mn | | |
|---|---|---|---|---|---|---|
| Energy term, kcal/mol | C1 | C7 | *c*-C4 | C1 | C7 | *c*-C4 |
| $\Delta E_{FRZ}$ | −12.3 | −13.1 | −13.3 | −7.8 | −8.7 | −9.4 |
| $\Delta E_{POL}$ | 4.4 | 5.2 | 5.7 | 2.4 | 3.0 | 3.6 |
| $\Delta E_{CT}$ | 21.7 | 23.3 | 25.5 | 15.2 | 16.8 | 18.7 |
| $\Delta E_{M\rightarrow A}/\Delta E_{CT}$, % | 26 | 24 | 25 | 30 | 28 | 27 |
| $\Delta E_{A\rightarrow M}/\Delta E_{CT}$, % | 74 | 76 | 75 | 70 | 72 | 73 |
| $\Delta E_{GD}$ | −3.4 | −2.9 | −4.1 | −1.7 | −1.5 | −2.2 |
| $\Delta E_{TOT} = \Delta E_{FRZ} + \Delta E_{POL} + \Delta E_{CT} + \Delta E_{GD}$ | 10.4 | 12.5 | 13.8 | 8.1 | 9.6 | 10.7 |

The energies reported here are not directly comparable to the binding energies reported in Fig. 3 because they do not include zero-point vibration energies.

occupied orbitals of the alkane to the vacant orbitals of the metal complex ($\Delta E_{A\rightarrow M}$), and the remainder is due to backbonding ($\Delta E_{M\rightarrow A}$). The stronger binding observed for the rhenium complexes appears to be due to a higher total amount of charge transfer, and not to different relative amounts of forward- and back-donation (Table 2).

## Conclusions

The main conclusions that should be drawn from this work are that the stability of an alkane $\sigma$-complex increases with the number of alkane–metal interaction sites, and that the binding interaction is primarily one of charge transfer, mostly from the alkane to the metal. Also, as expected, the manganese complex binding energies are significantly lower than those of their rhenium analogs; the lower BEs observed for the manganese complexes are due to lower amounts of total charge transfer, and not to different relative amounts of forward and back-donation, as compared with the rhenium complexes.

According to the calculations presented in this work, the binding energies for the binuclear complexes approach 20 kcal/mol; these complexes, once synthesized, are not likely to be stable at room temperature. Calculations are underway on a series of trinuclear complexes, which are expected to have higher BEs than the binuclear complexes, perhaps high enough to make them stable under ambient conditions. Also, there is some theoretical evidence that replacement of a $\pi$-accepting CO ligand, which is believed to compete with the alkane for the metal d electrons, by a pure $\sigma$-donor such as $NH_3$ increases the stability of alkane adducts (42). Calculations are in progress on a series of complexes with one or more of the CO ligands replaced by ammonia. Efforts are under way aimed at synthesizing some of the complexes examined in this paper. Future computational work will include further investigation of the effects of ligand identity on the strength of the metal–alkane interaction. The goal of such work will be to maximize the metal–alkane interaction, without actually causing activation of the C—H bond, by adjusting the amount of metal-to-alkane back-bonding.

## Methods

Each transition metal complex–alkane interaction energy was found by optimizing three structures, the entire alkane–transition metal complex, the transition-metal complex alone, and the alkane alone, and then subtracting the latter two energies from the first. In this work, favorable (negative) interaction energies are reported as positive binding energies.

The optimizations were performed first at the Hartree–Fock (HF) level (43), followed by a gradient-corrected DFT level optimization, using the exchange functional of Becke (36) and the correlation functional of Perdew (37), a combination known as BP86. The binding energies presented in this work are calculated at the BP86 level from the BP86-optimized structures. The BP86 functional combination is known for its consistently accurate predictions of the geometries, vibrational frequencies, and bond energies of transition metal complexes in general (44–47). It has also proven successful in the study of Group VI transition metal dihydrogen $\sigma$-complexes (48–50). For all calculations presented in this work, the 6–31G* basis set (51) was used for the non-metal atoms, and the LANL2DZ basis set and effective core potential (52) were used for rhenium and manganese.[§§] Vibrational frequencies and zero-point vibrational energies were calculated for the optimized structures. All optimized structures had zero imaginary frequencies[¶¶], indicating that they were minima on the potential energy surfaces. As recommended by Frenking *et al.* (14), the binding energies reported in this work have not been corrected for basis set superposition error (BSSE). However, the basis set superposition errors were estimated by using the standard counterpoise correction method (54), and are reported in SI Figs. 8 and 10. Cartesian coordinates, snapshots, and geometrical parameters of all complexes reported in this work are also provided in *SI Appendix*. Also, for the interested reader, structures and binding energies calculated at the Hartree–Fock (HF), DFT(B3LYP) (55), resolution-of-the-identity second-order Møller–Plesset perturbation theory (RIMP2) (56–61), and scaled opposite-spin MP2 (SOS-MP2) (62) levels of theory are also provided in SI Figs. 8–11.

ALMO EDA calculations were used to analyze the nature of the alkane–metal bond (41). The ALMO EDA calculations were performed without BSSE correction and without zero point vibrational energy corrections. The ALMO EDA calculations were performed using a developmental version of Q-CHEM; all other calculations reported in this work and in the SI were performed using either Q-CHEM 2.0 or Q-CHEM 3.0 (63, 64).

**Note added in proof:** For a review on the role of $\sigma$-complexes in $\sigma$-bond metathesis, see ref. 65.

We are grateful to Dr. Bernard R. Brooks, Director of the Laboratory of Computational Biology at the National Heart, Lung and Blood Institute of the National Institutes of Health for the use of the LoBoS cluster to perform the majority of the calculations reported in this work. This research was supported in part by the Intramural Research Program of the National Institutes of Health, National Heart, Lung,

[§§]Because the LANL2DZ basis set does not include polarization functions, the 6–31G*, LANL2DZ basis set combination is somewhat mismatched. The effects of this mismatch were investigated; the complex–alkane binding energies [at the BP86/(6–31G*, LANL2DZ)-optimized geometries] calculated with *f* functions (53) present on rhenium vary slightly (<1 kcal/mol) from those reported in this work.

[¶¶]One complex, [CpRe(CO)$_2$](*n*-pentane), had an imaginary frequency of magnitude 35 cm$^{-1}$. An imaginary frequency this small is considered most likely to be an artifact, not an indication that the structure that possesses it is a transition state.

and Blood Institute. This work was also supported by the Director, Office of Energy Research, Office of Basic Energy Sciences, Chemical Sciences Division of the U.S. Department of Energy under Contract no. DE-AC03-76SF00098. We thank Jamin Krinsky of the Bergman group, Rohini Lochan of the Head-Gordon group, and the reviewers and editor of this Special Feature for many helpful suggestions for improvements to the manuscript. We also acknowledge helpful discussions with Marty Lail, Mitchell Anstey, and Prof. Peter Vollhardt, who are working on the synthesis of some of the complexes described in this paper.

1. Bergman RG (1984) *Science* 223:902–908.
2. Labinger JA, Bercaw JE (2002) *Nature* 417:507–514.
3. Hall C, Perutz RN (1996) *Chem Rev* 96:3125–3146.
4. Wick DD, Reynolds KA, Jones WD (1999) *J Am Chem Soc* 121:3974–3983.
5. Crabtree RH (1995) *Chem Rev* 95:987–1007.
6. Periana RA, Bhalla G, Tenn WJ, Young KJH, Yang Liu X, Mironov O, Jones CJ, Ziatdinov VR (2004) *J Mol Cat A* 220:7–25.
7. Labinger JA (2004) *J Mol Cat A* 220:27–35.
8. Crabtree RH (2004) *J Organomet Chem* 689:4083–4091.
9. Geftakis S, Ball GE (1998) *J Am Chem Soc* 120:9953–9954.
10. Lawes DJ, Geftakis S, Ball GE (2005) *J Am Chem Soc* 127:4134–4135.
11. Lawes DJ, Darwish TA, Clark T, Harper JB, Ball GE (2006) *Angew Chem Int Ed* 43:4486–4490.
12. Castro-Rodriguez I, Nakai H, Gantzel P, Zakharov LN, Rheingold AL, Meyer K (2003) *J Am Chem Soc* 125:15734–15735.
13. Evans DR, Drovetskaya T, Bau R, Reed CA, Boyd PDW (1997) *J Am Chem Soc* 119:3633–3634.
14. Frenking G, Antes I, Böhme M, Dapprich S, Ehlers AW, Jonas V, Neuhaus A, Otto M, Stegmann R, Veldkamp A, Vyboishchikov SF (1996) in *Reviews in Computational Chemistry*, eds Lipkowitz KB, Boyd DB (VCH, New York), Vol 8, pp 63–144.
15. Cundari TR, Benson MT, Lutz ML, Sommerer SO (1996) in *Reviews in Computational Chemistry*, eds Lipkowitz KB, Boyd DB (VCH, New York), Vol 8, pp 145–202.
16. Ziegler T (1991) *Chem Rev* 91:651–667.
17. Furche F, Perdew JP (2006) *J Chem Phys* 124:044103–044127.
18. Perutz RN, Turner JJ (1975) *J Am Chem Soc* 97:4791–4800.
19. Turner JJ, Burdett JK, Perutz RN, Poliakoff M (1977) *Pure Appl Chem* 49:271–285.
20. Morse JM, Parker GH, Burkey TJ (1989) *Organometallics* 8:2471–2474.
21. Braslavsky SE, Heibel GE (1992) *Chem Rev* 92:1381–1410.
22. Leu G-L, Burkey TJ (1995) *J Coord Chem Soc* 34:87–95.
23. Yang GK, Vaida V, Peters KS (1988) *Polyhedron* 7:1619–1622.
24. Brown CE, Ishikawa Y, Hackett PA, Rayner PM (1990) *J Am Chem Soc* 112:2530–2536.
25. Buchanan JM, Stryker JM, Bergman RG (1986) *J Am Chem Soc* 108:1537–1550.
26. Periana RA, Bergman RG (1986) *J Am Chem Soc* 108:7332–7346.
27. Bullock RM, Headford CEL, Hennessy KM, Kegley SE, Norton JR (1989) *J Am Chem Soc* 111:3897–3908.
28. Parkin G, Bercaw JE (1989) *Organometallics* 8:1172–1179.
29. Gould GL, Heinekey DM (1989) *J Am Chem Soc* 111:5502–5504.
30. Bengali AA, Arndtsen BA, Burger PM, Schultz RH, Weiller BH, Kyle KR, Moore CB, Bergman RG (1995) *Pure Appl Chem* 67:281–288.
31. Arndtsen BA, Bergman RG, Mobley TA, Peterson TH (1995) *Acc Chem Res* 28:154–162.
32. McNamara BK, Yeston JS, Bergman RG, Moore BC (1999) *J Am Chem Soc* 121:6437–6443.
33. Bergman RG, Cundari TR, Gillespie AM, Gunnoe TB, Harman WD, Klinckman TR, Temple MD, White DP (2003) *Organometallics* 22:2331–2337.
34. Childs GI, Grills DC, Sun XZ, George MW (2001) *Pure Appl Chem* 73:443–447.
35. Childs GI, Colley CS, Dyer J, Grills DC, Sun XZ, Yang J, George MW (2000) *J Chem Soc Dalt Trans* 2000:1901–1906.
36. Becke AD (1988) *Phys Rev A* 38:3098–3100.
37. Perdew JP (1986) *Phys Rev B* 33:8822–8824.
38. Vetter AJ, Flaschenriem C, Jones WD (2005) *J Am Chem Soc* 127:12315–12322.
39. Bengali AA (2005) *J Organomet Chem* 690:4989–4992.
40. Childs GI, Colley CS, Dyer J, Grills DC, Sun XZ, Yang J, George MW (2000) *J Chem Soc Dalt Trans* 2000:1901–1906.
41. Khaliullin RZ, Head-Gordon M, Bell AT (2006) *J Chem Phys* 124:204105–204111.
42. Siegbahn PEM, Svensson M (1994) *J Am Chem Soc* 116:10124–10128.
43. Szabo A, Ostlund NS (1996) in *Modern Quantum Chemistry: Introduction to Advanced Electronic Structure Theory* (Dover, New York), pp 108–229.
44. Torrent M, Sola M, Frenking G (2000) *Chem Rev* 100:439–493.
45. Furche F, Perdew JP (2006) *J Chem Phys* 124:044103–044127.
46. Hyla-Kryspin I, Grimme S (1997) *Organometallics* 16:4807–4815.
47. Buhl M, Kabrede HJ (2006) *Chem Theory Comput* 2:1282–1290.
48. Kubas GJ (2001) *Metal Dihydrogen and ϛ-bond Complexes: Structure, Theory, and Reactivity* (Kluwer Academic/Plenum, New York)
49. Nemcsok DS, Kovacs A, Rayon VM, Frenking G (2002) *Organometallics* 21:5803–5809.
50. Li J, Ziegler T (1996) *Organometallics* 15:3844–3849.
51. Hariharan PC, Pople JA (1973) *Theor Chim Acta* 28:213-222.
52. Hay PJ, Wadt WR (1985) *J Chem Phys* 82:299–310.
53. Ehlers AW, Bohme M, Gobbi DA, Hollwarth VJ, Kobler KF, Stegmann R, Veldkamp A, Frenking G (1993) *Chem Phys Lett* 208:111–115.
54. Boys SF, Bernardi F (1970) *Mol Phys* 19:553–566.
55. Stephens PJ, Devlin FJ, Chabalowski CF, Frisch MJ (1994) *J Phys Chem* 98:11623–11627.
56. Feyereisen M, Fitzgerald G, Komornicki A (1993) *Chem Phys Lett* 208:359–363.
57. Weigend F, Haser M, Patzelt H, Ahlrichs R (1998) *Chem Phys Lett* 294:143–152.
58. DiStasio RA, Jung YS, Head-Gordon M (2005) *J Chem Theory Comput* 1:862–876.
59. DiStasio RA, Steele RP, Rhee YM, Shao Y, Head-Gordon M (2006) *Chem Phys Lett* 426:197–203.
60. Rhee YM, DiStasio RA, Lochan RC, Head-Gordon M (2007) *Chem Phys Lett*, in press.
61. Weigend F, Haser M (1997) *Theor Chem Acc* 97:331–340.
62. Jung Y, Lochan RC, Dutoi AD, Head-Gordon M (2004) *J Chem Phys* 121:9793–9802.
63. Kong J, White CA, Krylov AI, Sherrill CD, Adamson RD, Furlani TR, Lee MS, Lee AM, Gwaltney SR, Adams TR, *et. al.* (2000) *J Comp Chem* 21:1532–1548.
64. Shao Y, Fusti-Molnar L, Jung Y, Kussmann J, Ochsenfeld C, Brown ST, Gilbert ATB, Slipchenko LV, Levchenko SV, O'Neill DP, *et al.* (2006) *Phys Chem Chem Phys* 8:3172–3191.
65. Perutz RN, Sabo-Etienne S (2007) *Angew Chem Int Ed* 46:2578–2592.